Novel Dications with Unfused Aromatic Systems: Trithiophene and Trifuran Derivatives of Furimidazoline

Petr Bilik,[b] Farial Tanious,[b] Arvind Kumar,[b] W. David Wilson,[b] David W. Boykin,[b] Pierre Colson,[c] Claude Houssier,[c] Michael Facompré,[a] Christelle Tardy,[a] and Christian Bailly*[a]

We report the synthesis, interaction with DNA, topoisomerase II inhibition, and cytotoxicity of two novel unfused aromatic dications derived from the antimicrobial agent furimidazoline. The central diphenylfuran core of furimidazoline has been replaced with a trithiophene (DB358) or a trifuran (DB669) unit and the terminal imidazoline groups were preserved. The strength and mode of binding of the drugs to nucleic acids were investigated by complementary spectroscopic techniques including spectrophotometric, surface plasmon resonance, circular and linear dichroism measurements. The trifuran derivative forms intercalation complexes with double-stranded DNA, whereas the mode of binding of the trithiophene derivative varies depending on the drug/DNA ratio, as independently confirmed by NMR spectroscopic studies performed with $(A\text{-}T)_7$ and $(G\text{-}C)_7$ oligomers. Two-dimensional NMR data provided a molecular model for the binding of DB358 within the minor groove of the AATT sequence of the decanucleotide $d(GCGAATTCGC)_2$. DNase I footprinting experiments confirmed the sequence-dependent binding of DB358 to DNA. The trithiophene derivative interacts preferentially with AT-rich sequences at low concentrations, but can accomodate GC sites at higher concentrations. DNA relaxation assays revealed that DB358 stimulated DNA cleavage by topoisomerase II, in contrast to DB669. The substitution of N*-alkylamidines for the imidazoline terminal groups abolished the capacity of the drug to poison topoisomerase II. At the cellular level, flow cytometry analysis indicated that DB358, which is about six times more cytotoxic than the trifuran analogue, induced a significant accumulation of HL-60 human leukemia cells in the G2/M phase. The incorporation of thiophene heterocycles appears as a convenient procedure to limit the strict AT selectivity of dications containing an extended unfused aromatic system and to design cytotoxic DNA intercalating agents acting as poisons for human topoisomerase II.*

KEYWORDS:

DNA recognition · drug research · heterocycles · surface plasmon resonance · topoisomerase II

Introduction

The diphenylfuran derivative furimidazoline (DB60) was initially designed as an antimicrobial agent derived from furamidine (DB75) (Scheme 1). Diphenylfurans hold promise to treat *Pneumocystis carinii* pneumonia (PCP) and other opportunistic infections which often afflict immune-compromised populations, in particular patients with acquired immune deficiency syndrome (AIDS).[1–5] But in addition to their antimicrobial properties, DB60 and related compounds have shown significant antiproliferative activities against various tumor cell lines, including cells resistant to cisplatinum.[6]

The pharmacological activities of diphenylfurans and related dications have been linked to their capacity to interact with DNA.[7, 8] These drugs bind to the minor groove of DNA and engage contacts with the edges of A·T base pairs. A pronounced selectivity for AT-rich sequences has been clearly demonstrated by footprinting studies and complementary spectroscopic measurements. But the situation is slightly different with DB60. We have shown that the substitution of the terminal imidazoline moieties of DB60 for the amidine moieties of DB75 markedly affects the sequence recognition process. Unlike other related compounds possessing *N*-alkylamidines, DB60 can form intercalation complexes at GC sites, in addition to forming minor-groove complexes at AT sites.[9] As a result, DB60 forms stable complexes with AT sites at low concentrations, but at higher concentrations the binding becomes totally nonspecific due to additional intercalation of drug molecules into GC-rich sequences.[10]

[a] *Dr. C. Bailly, M. Facompré, C. Tardy*
INSERM U-524 et Laboratoire de Pharmacologie Antitumorale du Centre Oscar Lambret, IRCL
Place de Verdun, 59045 Lille (France)
Fax: (+33) 3-20-16-92-29
E-mail: bailly@lille.inserm.fr

[b] *P. Bilik, F. Tanious, A. Kumar, Prof. W. D. Wilson, Prof. D. W. Boykin*
Department of Chemistry
Georgia State University
Atlanta, GA 30303 (USA)

[c] *Prof. P. Colson, Prof. C. Houssier*
Laboratoire de Chimie Macromoléculaire et Chimie Physique
Université de Liège au Sart-Tilman
4000 Liège (Belgium)

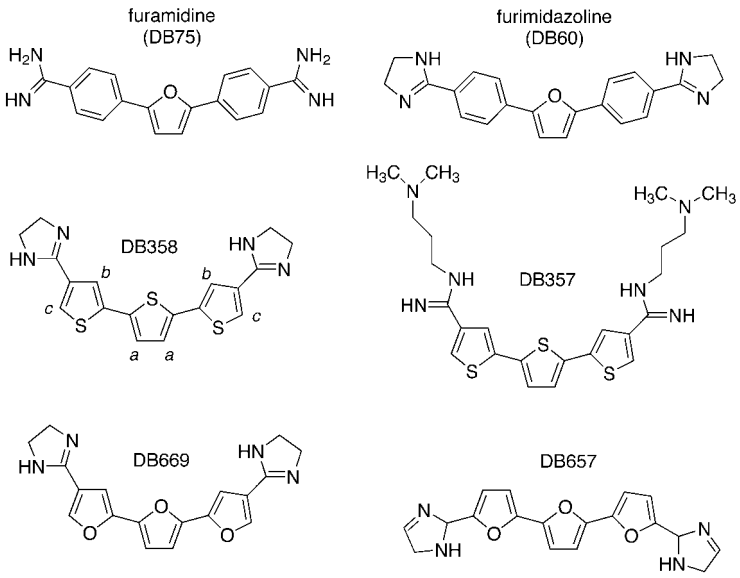

Scheme 1. *Structures of the drugs mentioned in this study (furamidine (DB75), furimidazoline (DB60), DB358, DB669, DB357, DB657). Hydrogen atoms of DB358 are labeled for discussion of the NMR spectroscopy experimental results.*

In addition, we discovered that DB60 was a poison for human topoisomerase II and this effect correlated with its ability to intercalate into DNA.[10] Thus DB60 bears unusual sequence-dependent recognition properties and as such it represents a useful template for the development of analogues endowed with different sequence recognition properties and perhaps with superior cytotoxic potential. In this context, here we report the design of two novel analogues, DB358 and DB669 containing three adjacent thiophene or furan heterocycles (Scheme 1). The replacement of the central diphenylfuran core of DB60 with a trithiophene or a trifuran unit preserves the overall crescent-shape geometry of the molecules, but the substitution of the extended unfused aromatic system may alter the hydrogen-bonding capabilities of the system. The central aromatic system of these dications is a key element for DNA sequence recognition. For example, in the amidine series, the replacement of the diphenylfuran moiety with a phenyl-furan-benzimidazole structure affords a compound capable of forming tight complexes with GC-containing sequences through the formation of dimeric motifs.[11] But here we kept the terminal imidazoline groups, which facilitate the intercalation process.[9]

Results

Chemical syntheses

The trithiophene DB358 was prepared in five steps starting from 4-bromothiophene-2-carboxaldehyde (**1**) (Scheme 2). The 1,4-diketone **2** was obtained by using Stetter chemistry.[12] Lawesson's reagent was employed to convert 1,4-diketone into the corresponding dibromotrithiophene **3**.[13] The corresponding bisnitrile **4** was obtained by the action of copper(I) cyanide in quinoline under reflux by using a standard procedure.[1] The bisnitrile **4** was converted into the bisimidazoline DB358 in a two-step process which involves a Pinner-type formation of the bisimidate ester salt followed by heating with ethylenediamine.[1] The overall yield for formation of DB358 was 9.5%.

The trifuran DB669 was prepared in three steps starting from 2,5-bis(tri-*n*-butylstannyl)furan and 2-bromo-4-cyanofuran (Scheme 3). The trifuran dinitrile **5** was obtained in 76% yield from a Stille coupling reaction.[14] The dinitrile was converted into the corresponding bisimidazoline by using the same two-step process described for the trithiophene analogue. The overall yield for formation of DB669 was 47%.

Interaction with DNA

A panel of complementary biophysical and biochemical approaches was deployed to examine successively the affinity, mode of binding to DNA, and sequence preference of DB358 and DB669. These three aspects are presented in the following sections.

DNA affinity: Thermal melting studies for DB358 and DB669 were done with poly(dA)·(dT), poly(dA-dT)$_2$, and calf thymus DNA. The ΔT_m (T_m of the drug–DNA complex minus T_m of the DNA alone) values collated in Table 1 show interesting differences between the thiophene and furan compounds. With the AT polymers and DB358 the melting temperature is significantly higher than with the furan derivative. In contrast, the measurement with calf thymus DNA shows very similar results for the two

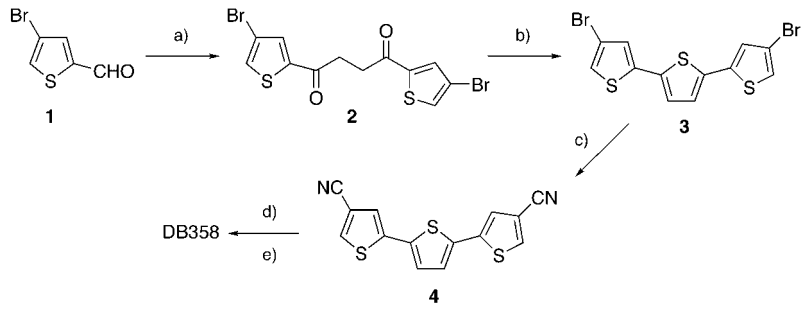

Scheme 2. *Synthesis of the trithiophene DB358. a) Divinyl sulfone, 3-benzyl-5-hydroxyethyl-4-methylthiazolium chloride, NaOAc, EtOH; b) Lawesson's reagent; c) CuCN; d) HCl, EtOH; e) $NH_2CH_2CH_2NH_2$, EtOH.*

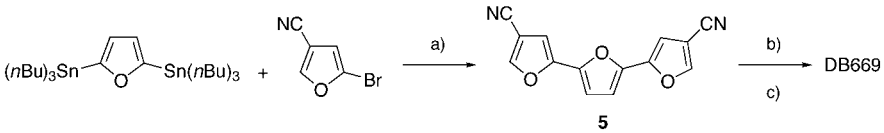

Scheme 3. *Synthesis of the trifuran DB669. a) [Pd(PPh$_3$)$_4$], dioxane; b) HCl, EtOH; c) $NH_2CH_2CH_2NH_2$, EtOH.*

Table 1. *Results of thermal melting studies with free and complexed DNA probes.*[a]

DNA	Ligand			
	free DNA (T_m)	DB358 (ΔT_m)	DB669 (ΔT_m)	DB60 (ΔT_m)
poly(dA)·(dT)[b]	66.9	24.0	6.5	25
poly(dA-dT)$_2$[b]	59.3	16.5	8.0	24.5
calf thymus DNA[c]	57.8	26.0	24.0	28.2

[a] T_m and ΔT_m (T_m of the drug–DNA complex minus T_m of the free DNA) values are given in °C. [b] T_m measurements were performed in MES (2-(*N*-morpholino)ethanesulfonic acid) buffer (0.01 M MES and 1 mM EDTA) containing 0.1 M NaCl. [c] T_m measurements were performed in MES buffer without NaCl.

compounds. To obtain additional information about the interaction of the strong-binding trithiophene compound with different DNA sequences, its interaction with three hairpin oligomers was determined by surface plasmon resonance (SPR) methods (Figure 1). All binding curves were fit by nonlinear least squares to a model that assumed three approximately equal binding sites on the oligomers. Three sites are required by the magnitude of the SPR signal at high compound concentration. More complex fitting models did not result in any significant

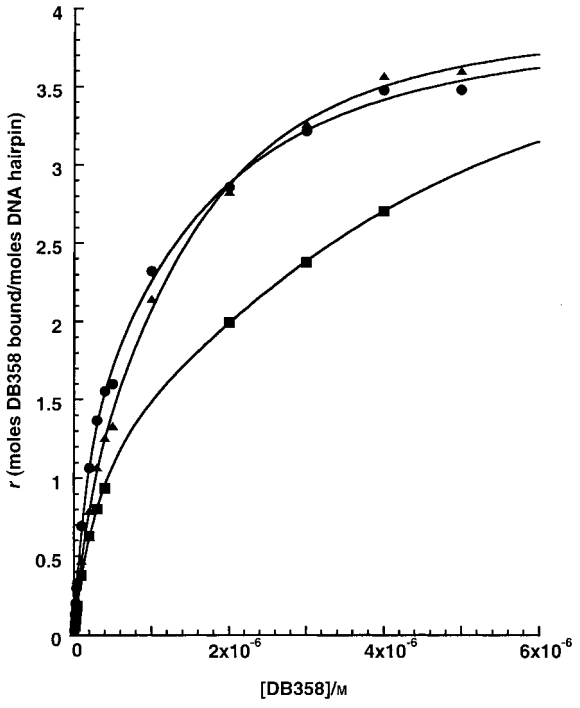

Figure 1. *Determination of the affinity constants by SPR for DB358 complexed with AATT (▲), AT (●), and GC (■) sites. The experiment was conducted in MES buffer containing 0.1 M NaCl at 25 °C. The r values were determined by using Equation (1) and the RU values from the steady-state region of the sensorgrams.*[21] *The r values are plotted versus the concentration of unbound DB358. The results were fit by nonlinear least-squares methods to a three-site model [Eq. (1)]. The hairpin DNA sequences are as follows: AATT = 5′-biotin-CGAATTCGCTCTCGAATTCG-3′; AT = 5′-biotin-CATATATATCCCCATATATATG-3′; GC = 5′-biotin-CGCGCGCGTTTTCGCGCGCG-3′. The hairpin loop sequences are underlined.*

improvement in the quality of the fit. The binding constants obtained for DB358 were $1.7 \times 10^6\,M^{-1}$ for the alternating AT oligomer, $1.4 \times 10^6\,M^{-1}$ for the AATT sequence, and $0.6 \times 10^6\,M^{-1}$ for the alternating GC sequence. The compounds thus exhibit a slight AT specificity.

Mode of binding: The different behaviors of DB358 and DB669 were also evident from the spectrophotometric analysis performed with the alternating polynucleotides poly(dA-dT)$_2$ and poly(dG-dC)$_2$. Both compounds have strong absorption bands in the 300–400-nm spectral region and the absorption spectra are strongly perturbed when the drugs form complexes with DNA. Titration of DB358 with poly(dA-dT)$_2$ (Figure 2a) shows changes that suggest more than one type of binding mode. Up to a ratio of [drug]/[DNA] = 0.5 there is a decrease in compound absorbance and one isosbestic point, but when the concentration of the DNA increases there is an increase in absorbance and a shift of the absorption maximum from 351 to 363 nm. The spectral changes are much larger on titration with the GC sequence (Figure 2b), but there is still no isosbestic point. Up to the ratio of [drug]/[DNA] = 0.5, there is a decrease in compound absorbance and one isosbestic point. Above this ratio a strong shift of the absorption maximum (from 351 to 369 nm) is observed with no significant increase in compound absorption. Titration of DB669 shows decreases in absorbance and isosbestics points over the whole range of concentrations for both polymers. The decrease in absorbance is slightly larger during the titration with the GC polynucleotide than with the AT sequence (Figures 2c and 2d).

The compounds have no circular dichroism (CD) spectrum when free in solution, but have induced CD spectra in their nucleic acid complexes. Titration of poly(d(A-T)$_2$) with DB358 (Figure 3a) shows significant increases in ellipticity both in the DNA 260-nm band and in the drug absorption regions. The negative band at 230–240 nm became more negative in the drug complex. There are two induced peaks in the drug absorption region with peaks at 315 and 375 nm. There is no induced CD on titration with poly(d(G-C)$_2$) under the same conditions. At low salt concentration and high ratios of compound to DNA, a weak induced peak with maximum at 390 nm was seen (data not shown). CD titrations of poly(d(G-C)$_2$) with DB669 also indicated no changes of ellipticity in the whole studied range of ratios in MES buffer. Titration of poly(d(A-T)$_2$) with DB669 shows practically no changes of the CD spectrum in the DNA region but a small broad induced peak at 330 nm in the compound absorption region (Figure 3b).

The electric linear dichroism (ELD) spectra of DB358 and DB669 bound to calf thymus DNA are presented in Figure 4a. In both cases, the reduced dichroism $\Delta A/A$ is negative in the drug absorption band. In contrast to conventional minor-groove binders such as furamidine, no positive signal was obtained. For DB669, the 310–350-nm negative band reflects the orientation of the drug chromophore along the electric field. The fact that $\Delta A/A$ depends almost similary upon the field strength for the DB669–DNA complex at 340 nm and the DNA bases at 260 nm in the absence of ligand (Figure 4b) suggests that the drug chromophore is oriented parallel to the DNA base pairs, as expected for an intercalative binding. The situation is more

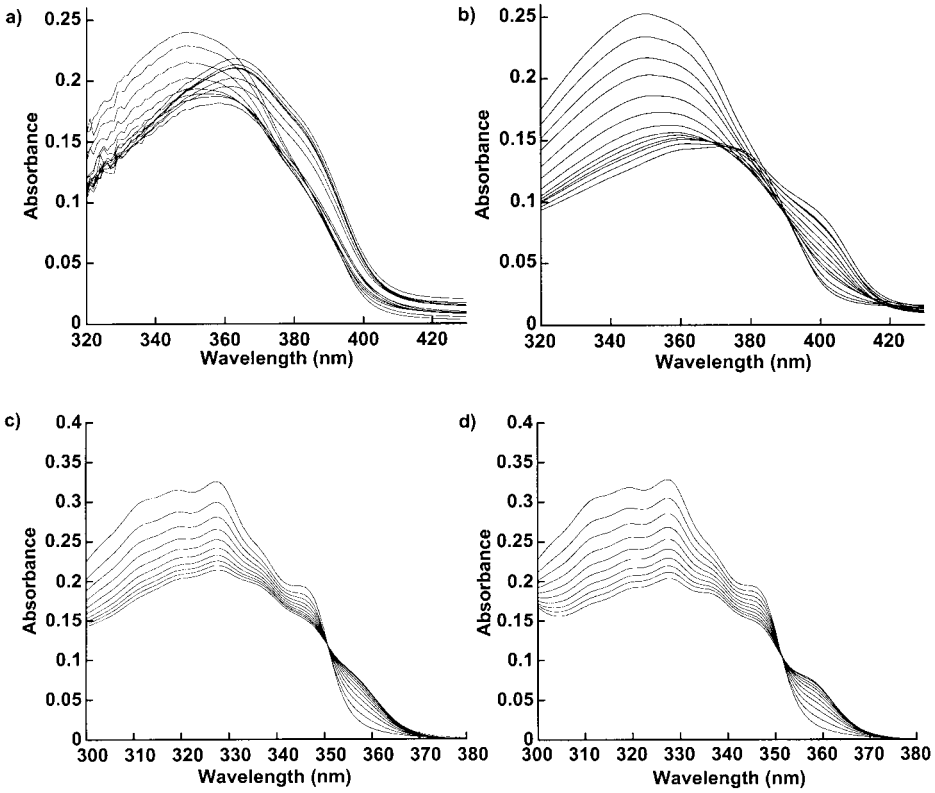

Figure 2. Spectrophotometric titration of DB358 with poly(d(A-T)$_2$) (A) and poly(d(G-C)$_2$) (B). a) Concentrations used: 1.3×10^{-5} M of DB358 and poly(d(A-T)$_2$) concentrations (in base pairs) of 0, 2.19×10^{-6}, 4.79×10^{-6}, 8.63×10^{-6}, 1.28×10^{-5}, 1.69×10^{-5}, 2.10×10^{-5}, 2.49×10^{-5}, 3.26×10^{-5}, 4.00×10^{-5}, 4.72×10^{-5}, 5.41×10^{-5}, 6.08×10^{-5}, and 6.72×10^{-5}, respectively, from the top to the bottom curves at 351 nm. b) Concentrations used: 1.3×10^{-5} M of DB358 and poly(d(G-C)$_2$) concentrations (in base pairs) of 0, 1.28×10^{-6}, 3.81×10^{-6}, 6.31×10^{-6}, 9.37×10^{-6}, 1.30×10^{-5}, 1.53×10^{-5}, 1.99×10^{-5}, 2.71×10^{-5}, 3.24×10^{-5}, 3.76×10^{-5}, 4.25×10^{-5}, 4.73×10^{-5}, and 5.19×10^{-5}, respectively, from the top to the bottom curves at 351 nm. c) and d) Spectrophotometric titration of DB669 with poly(d(A-T)$_2$) and poly(d(G-C)$_2$), respectively. The concentrations used were the same for both titrations: 1.3×10^{-5} M of DB669 and DNA concentrations (in base pairs) of 0, 8.63×10^{-6}, 1.69×10^{-5}, 2.49×10^{-5}, 3.26×10^{-5}, 4.00×10^{-5}, 4.72×10^{-5}, 5.41×10^{-5}, 6.08×10^{-5}, and 6.72×10^{-5}, respectively, from the top to the bottom curves at 327 nm.

complex with DB358, which only gives weakly negative reduced dichroism signals. Similar spectra with $\Delta A/A$ values of about -0.12 were obtained when using AT or GC polynucleotides (data not shown). For DB358, it is likely that two populations coexist, one bound to the minor groove and the other intercalated into the double helix. Similar complicated ELD data were previously obtained with DB60 bound to calf thymus DNA.[9]

NMR studies were conducted with DB358 in order to further evaluate the interaction mode. Basic 1D-NMR studies have been done with (A-T)$_7$ and (G-C)$_7$ oligomers. Titration with the (A-T)$_7$ oligomer was studied at ratios of [DNA]/[drug] = 0, 0.5, 1, 2, 3, 4, and 5 at 50 °C, which offered the best resolution. Within the ratio range 0–2 large upfield shifts (lower δ) of the thiophene peaks were observed (7.255 →6.715 (a); 7.513 →7.135 (b); 8.201 →7.975 (c); see Scheme 1 for hydrogen atom labeling), consistent with intercalation. With the higher ratio range slight downfield shifts were observed (6.762 (a); 7.161 (b); 8.000 (c)), consistent with groove binding. The chemical shift of the imidazoline methylene groups remained constant in the whole range of the ratios. NMR spectra with the (G-C)$_7$ oligomer were obtained at three different ratios, [DNA]/[drug] = 0, 1, and 3 at 70 °C (precipitation occurred at higher ratios). Larger upfield shifts of thiophene peaks (7.255 →6.529 (a); 7.513 →7.052 (b); 8.201 →7.862 (c)) were obtained than during titration with the (A-T)$_7$ oligomer. The imidazoline methylene group signals shifted slightly upfield from $\delta = 4.007$ to $\delta = 3.979$.

1D-NMR studies with d(GCGAATTCGC)$_2$, which has been used in the study of a number of similar dications, were done as a function of temperature in order to find appropriate conditions for 2D-NMR studies with this sequence. The best resolution was obtained at 35 °C, and a 1D-NMR titration is shown in Figure 5. Large downfield shifts of thiophene peaks (7.255 →7.535 (a); 7.513 →7.661 (b); 8.201 →8.393 (c)) are observed, whereas the position of the methylene proton signals of the imidazoline moieties remained almost the same. 2D-NOESY NMR spectra in D_2O (Figure 6a) showed a cross peak between the b-hydrogen atoms of DB358 and the T6-H1′ hydrogen atom of DNA. A cross peak between the b-hydrogen atoms of the drug and the A5-H2 hydrogen atom was observed in the aromatic region (Figure 6b). All of these cross peaks are consistent with minor-groove binding of the compound in the AATT sequence at ratios of 1:1 and below. DB358 was visually docked into the minor groove of the AATT sequence of the d(GCGAATTCGC)$_2$ decamer (Figure 7). Prior to docking it was necessary to rotate the thiophene rings into suitable positions. The compound fits into the minor groove and can form hydrogen bonds between imidazoline hydrogen atoms and thymine O2 atoms as shown in Figure 7. It was also clearly possible to see that all hydrogen atoms involved in observed NOESY interactions are within distances to explain the observed cross peaks.

Sequence selectivity: Footprinting studies were performed using the endonuclease DNase I, which is a sensitive enzyme for mapping DNA-binding sites of small molecules.[15] Two 3′-end-labeled DNA restriction fragments of 117 and 265 base pairs, cut out from the plasmid pBS, were used as substrates. A typical autoradiograph of a sequencing gel used to fractionate the products of partial digestion of the 117-mer complexed with DB358 and DB669 is presented in Figure 8a. With DB669 there was relatively little inhibition of DNase I cutting, whereas DB358 affected the cleavage of the fragment by the nuclease more

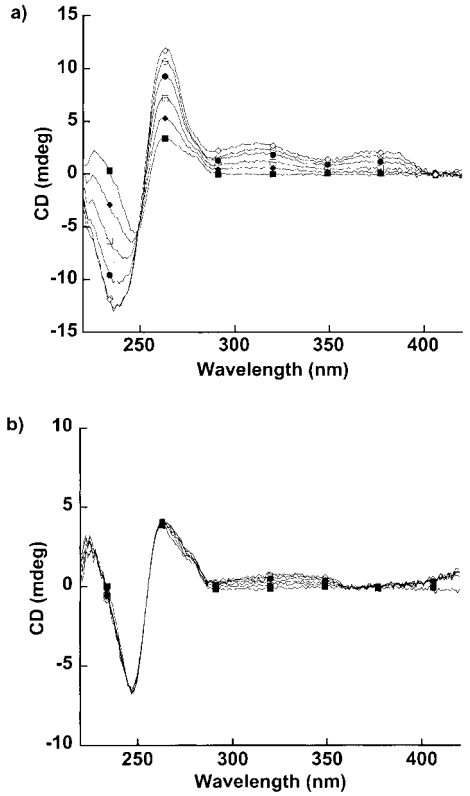

Figure 3. *CD spectra of DB358 (a) and DB669 (b) with poly(d(A-T)$_2$). Experiments were conducted in a 1-cm cell in MES buffer with 0.1 M NaCl added at 25 °C at a DNA concentration of 2.5 × 10^{-5} M (in base pairs). The ratios of compound/poly(d(A-T)$_2$) (in base pairs) are 0 (■), 0.05 (◆), 0.10(□), 0.15 (●), 0.20 (○), and 0.25 (◇) (a) and 0 (■), 0.10 (◆), 0.20(□), 0.30 (●), 0.40 (○), and 0.50 (◇) (b).*

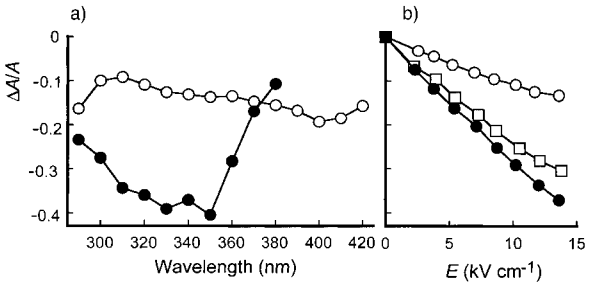

Figure 4. *Dependence of the reduced dichroism ΔA/A on a) the wavelength and b) the electric field strength for DB669 (●) and DB358 (○) bound to calf thymus DNA, at a DNA/drug ratio of 25 (250 μM DNA, 10 μM drug; □ = DNA alone). Conditions: a) 13.6 kV cm^{-1}, b) 360 nm for DB358, 340 nm for DB669, and 260 nm for DNA alone, in 1 mM sodium cacodylate buffer, pH 7.0.*

efficiently. A densitometric analysis of the 0.5-μM lanes is presented in Figure 9a. In the presence of DB358, four regions of attenuated DNA cleavage can be discerned around positions 25, 44, 64, and 84, corresponding to the sequences 5′-TTGTAA, 5′-TAAA, 5′-TTTCC, and 5′-TAAGT, respectively. DB669 showed no such protection of AT-rich sequences. For concentrations $\leq$ 1 μM, DB358 protects AT sites from cutting by DNase I, but at higher concentrations ($\geq$ 2 μM), the drug inhibits DNA cleavage all along the fragment. A similar effect was seen with 5 μM DB669 and was

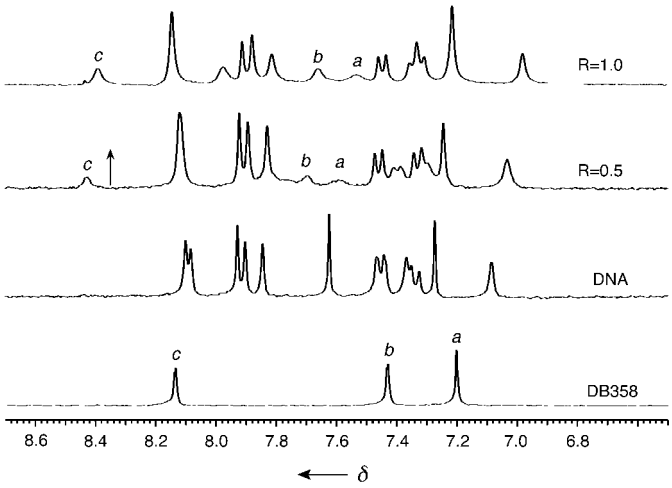

Figure 5. *1D-NMR titration of the d(GCGAATTCGC)$_2$ decamer duplex with DB358 at 35 °C (only the aromatic region is shown). The concentration of duplex DNA was 0.5 mM. R refers to the [drug]/[DNA] ratio. Peaks corresponding to the thiophene hydrogen atoms are labeled according to Scheme 1.*

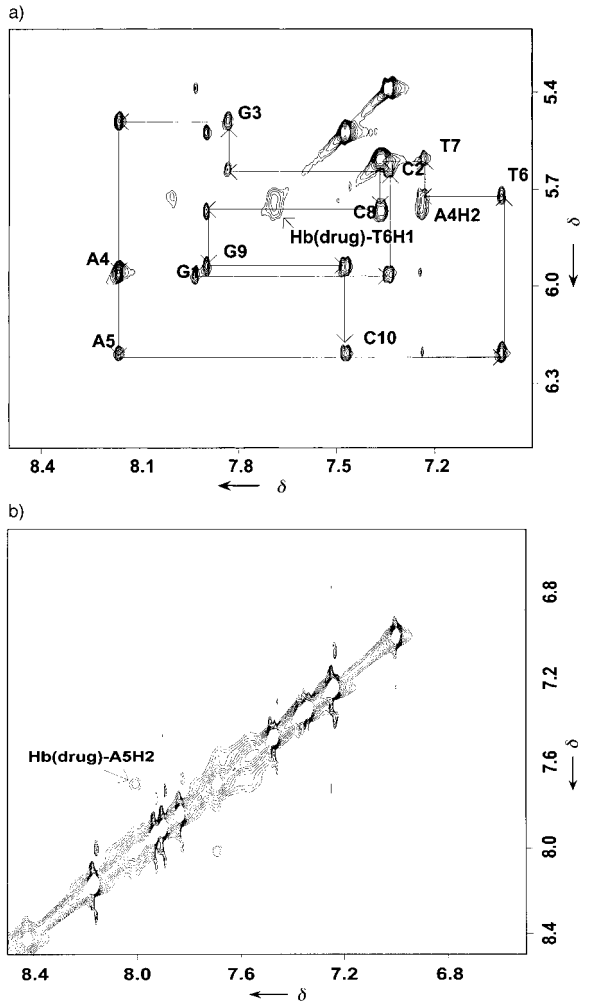

Figure 6. *a) Expanded aromatic proton 300-ms NOESY NMR spectrum at 35 °C showing cross peak Hb/T6H1′ between DB358 and the AATT decamer. b) Expanded phase-sensitive 300-ms NOESY NMR aromatic proton spectrum at 25 °C showing cross peak Hb/A5H2 between DB358 and the AATT decamer.*

Figure 7. *Molecular model of the trithiophene DB358 docked into the AATT site in the minor groove of the d(GCGAATTCGC)$_2$ decamer. Atoms for DB358 are colored according to atom types: carbon = white, hydrogen = cyan, nitrogen = blue, and sulfur = yellow. The two DNA strands are shown in purple and green for visualization.*

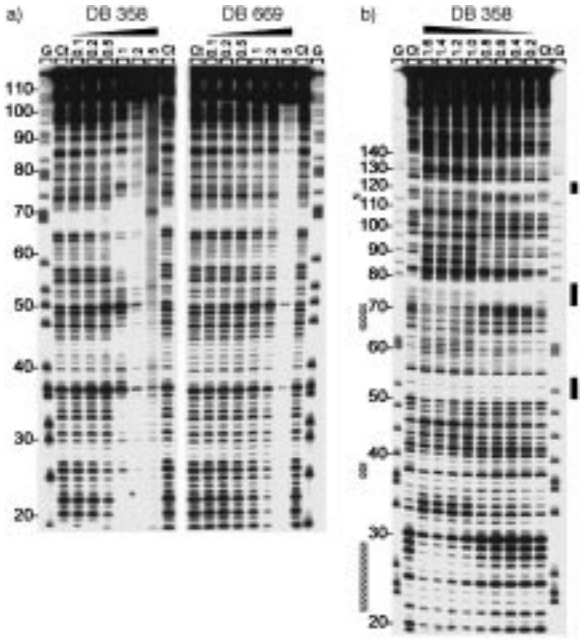

Figure 8. *DNA footprinting gels showing sequence-selective binding of the drugs to a) the 117-mer and b) the 265-mer* PvuII – EcoRI *restriction fragments cut from the plasmid pBS. The drug concentrations (in μM) are indicated at the top of each lane. The products of DNase I digestion were resolved on 8% (w/v) polyacrylamide gels containing 8 M urea. Control tracks (Ct) contained no drug. Guanine-specific sequence markers obtained by treatment of the DNA with dimethylsulfate followed by piperidine were run in the lanes marked G. Numbers on the side of the gel refer to the standard numbering scheme for the nucleotide sequence of the DNA fragment, as indicated in Figure 9. For the gel in Figure b, bars indicate the sites of reduced cleavage by DNase I in the presence of DB358 bound to the 265-mer fragment.*

previously reported with DB60. This effect is connected with the ability of the imidazoline compounds to form intercalation complexes.[10]

Similar results were obtained with the 265-mer fragment. DB669 poorly inhibited DNase I cleavage, whereas low concentrations of DB358 produced footprints mainly at AT sites. But we noted that with DB358 different footprinting patterns were generated depending on the drug concentration. The sequence recognition properties of DB358 are manifestly concentration-dependent. This can be clearly seen in the gel in Figure 8 b and the corresponding differential cleavage plots in Figure 9 b.

At 0.4 μM DB358 protects cleavage of the 265-mer by DNase I at two sites around positions 53 and 76. Both regions correspond to AT-rich sites (5′-AAAA and 5′-ATTAA). But as the drug concentration increases, the magnitude of the footprints at these AT tracts decreases and new binding sites appeared around positions 28, 40, 50, and 71. These new sites are composed of both A·T and G·C base pairs. The 5′-TCTAG site around position 28 provides a favored receptor for DB358 at 1.6 μM (Figure 9 b). Therefore, the results of the footprinting experiments indicate clearly that DB358 interacts preferentially with AT sites at low concentrations but can accommodate GC sites at higher concentrations. This is in perfect agreement with the spectroscopic data showing that this trithiophene derivative displays different modes of binding to AT and GC sequences. It is interesting to note also that the

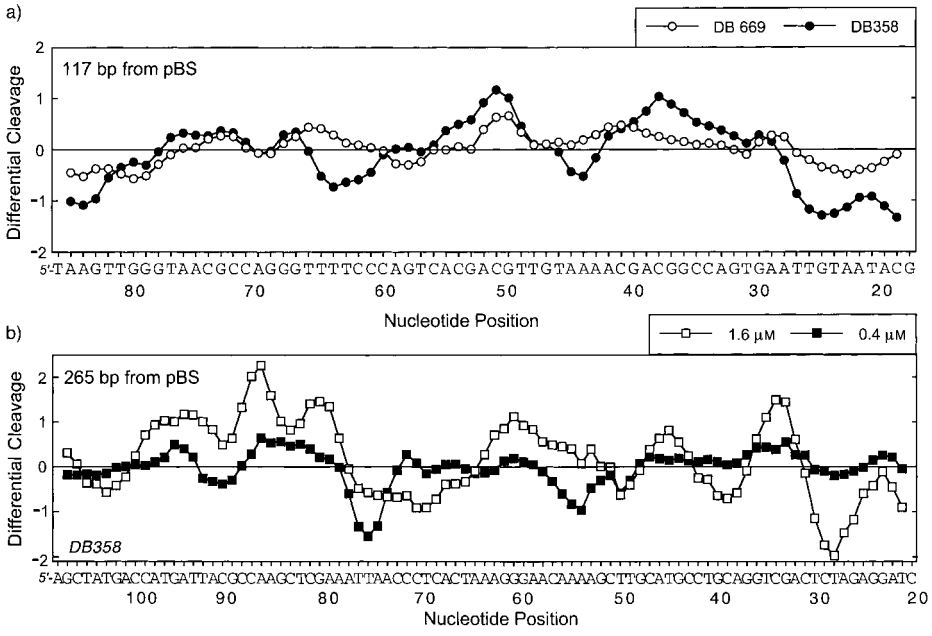

Figure 9. *Differential cleavage plots comparing the susceptibility of a) the 117-bp and b) the 265-bp fragments to DNase I cutting in the presence of DB358 or DB669. The plots in a) compare the effects of the two drugs at 0.5 μM concentration. The plots in b) show the different effects of DB358 at 0.4 μM or 1.6 μM concentration. Deviation of points towards the lettered sequence (negative values) corresponds to a ligand-protected site and deviation away from it (positive values) represents enhanced cleavage. Vertical scales are in units of $\ln(f_a) - \ln(f_c)$, where f_a is the fractional cleavage at any bond in the presence of the drug and f_c is the fractional cleavage of the same bond in the control, given a closely similar extent of digestion in each case.*

regions of enhanced cleavage by DNase I are more pronounced when DB358 binds to GC-containing sequences (at 1.6 μM) than when it binds primarily to AT sites (at 0.4 μM). Intercalation (at GC sites) is expected to induce larger perturbations of the double-helical structure of DNA than minor-groove binding (at AT sites).

Topoisomerases inhibition

A DNA relaxation assay was used to investigate the effects of the drugs on the catalytic activities of purified human topoisomerases I and II. In both cases, closed circular DNA was treated with the enzyme in the presence of increasing concentrations of the drugs and the DNA relaxation and cleavage products were analyzed by agarose gel electrophoresis. Neither DB358 nor DB669 act as poisons for topoisomerase I. In contrast to camptothecin used as a positive control, the band intensity of nicked DNA was not enhanced in the presence of the drugs (data not shown). On the contrary, a marked effect was observed with topoisomerase II. As shown in Figure 10, an intense band

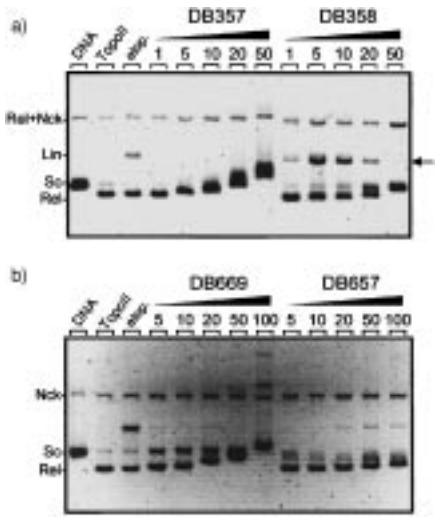

Figure 10. *Effect of increasing concentrations of a) DB357 and DB358, and b) DB657 and DB669 on the relaxation of plasmid DNA by human topoisomerases II. Native supercoiled pKMp27 DNA (0.5 μg) (lane "DNA") was incubated with four units of topoisomerase II in the absence (lane "TopoII") or presence of the drugs at the indicated concentration (in μM). Etoposide (lane "etop.") were used at 20 μM. Reactions were stopped with sodium dodecylsulfate and treatment with proteinase K. DNA samples were separated by electrophoresis on an agarose gel containing ethidium bromide (1 μg mL^{-1}). The gel was photographed under UV light. Nck = nicked, Lin = linear, Rel = relaxed, Sc = supercoiled.*

corresponding to linear DNA is produced in the presence of DB358. This reflects either the drug-induced stimulation of DNA cleavage by topoisomerase II or the inhibition of DNA religation. In the presence of DB358, the enzyme may stay longer on the DNA, thereby producing more double-strand breaks. The amount of double-strand breaks produced by topoisomerase II in the presence of DB358 is even superior to that obtained with the antitumor drug etoposide, which was used as a positive control. At 5 – 10 μM DB358 massively promotes DNA cleavage. Yet at higher concentrations (20 and 50 μM), a marked inhibition of cleavage is observed. This is a typical effect for an intercalating agent. Under the same conditions, DB669 did not enhance DNA cleavage. At high concentrations, DB669 inhibits DNA relaxation by topoisomerase II but failed to stimulate DNA cleavage. The strong inhibition of DNA relaxation observed with DB669 (and to a lower extent with DB358) is nonspecific and is without doubt a consequence of its intercalative binding to DNA.

Two related compounds were tested in the DNA relaxation assay (Figure 10). DB357 is an analogue of DB358 bearing dimethylaminopropylamidine side chains in place of the imidazoline groups. DB657 is a regioisomer of DB669 having the two imidazoline moieties at position 2 on the furan rings (Scheme 1). Interestingly, the substitution of *N*-alkylamidines for the imidazolines of DB358 prevented the poisoning of topoisomerase II. Conversely, relocation of the imidazolines of DB669 from the 1- to the 2-position restored a weak but noticeable capacity for the trifuran drug to stabilize covalent DNA – topoisomerase II complexes. The effect of DB657 is comparable to that seen previously with furimidazoline.[10] The strong stimulation of topoisomerase II-mediated DNA cleavage by DB358 is directly attributable to the presence of the terminal imidazoline groups, which are the only substituents that distinguish compounds DB357 and DB358. DB669 apparently does not act as a poison for topoisomerase II, but, however, it can inhibit the relaxation enzyme due to its strong interaction with DNA. The position of the imidazoline rings on the five-membered heterocycle must play a decisive role in the stabilization of the topoisomerase II – DNA complex.

Cytotoxicity and cell cycle effects

Treatment of human leukemia HL-60 cells with increasing concentrations of DB358, but not with DB669, for 24 hours led to profound changes of the cell cycle profiles (Figure 11). The

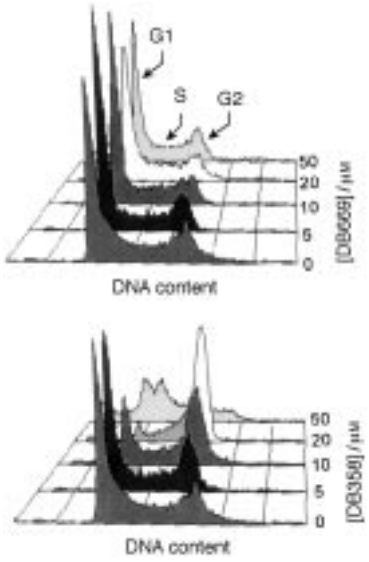

Figure 11. *Cell cycle analysis of HL-60 human leukemia cells treated with graded concentrations of DB669 (top) and DB358 (bottom) for 24 h. Cells were analyzed with the FACScan flow cytometer as described in the Experimental Section.*

flow cytometric analysis of propidium iodide labeled cells indicates that the treatment with 10 μM DB358 induces a significant accumulation of cells in the G2/M phase. The G2-cell population increases from 16% in the control to 92% in the presence of 20 μM DB358. Concomitantly, the G1-phase cell populations gradually decrease, and at a high concentration (50 μM) we started to detect cells with a DNA content less than that found in G1. Sub-G1 cells are usually considered as apoptotic cells.[16] No such effects were observed with DB669. With the trifuran compound, the cell cycle profiles remained unchanged, even when using a high drug concentration.

A conventional tetrazolium-based MTS assay was applied to determine the drug concentration required to inhibit cell growth by 50% after incubation in the culture medium for 72 hours. The calculated IC_{50} values with the HL-60 human leukemia cell line are 8.2 ± 0.7 μM and 51 ± 4 μM for DB358 and DB669, respectively. The trithiophene derivative is thus about seven times more cytotoxic than the trifuran analogue, but the cytotoxicity remains very modest compared to conventional anticancer drugs. For example, the same test performed with etoposide gave an IC_{50} value of 0.07 μM. Furimidazoline is slightly less toxic to HL-60 cells than DB358 ($IC_{50} = 11 \pm 1.2$ μM).

Discussion

The study shows that the substitution of a trithiophene or a trifuran unit for the unfused aromatic diphenylfuran system of furimidazoline (DB60) modifies significantly the DNA-binding properties of the dications thereby affecting their topoisomerase II inhibition and cytotoxic properties. We have previously demonstrated that DB60 displays two mechanisms of interaction with DNA depending on the target sequence. The bisimidazoline diphenylfuran compound forms minor-groove complexes with AT-rich sequences. In addition, DB60 can form intercalation complexes at GC sites.[9] However, the drug exhibits a marked minor groove/AT preference. The binding constant for DB60 to poly(d(A-T)$_2$) is 305 times higher than the binding constant to poly(d(G-C)$_2$).

Both the dual binding mode and sequence preference are considerably altered upon replacement of the phenyl rings of DB60 with furan rings. In sharp contrast to furimidazoline, DB669 appears to exhibit a single mode of interaction with DNA by intercalation. This change of the binding mechanism abolishes the capacity of the drug to recognize preferentially AT-rich sequences, as is the case with the vast majority of dications containing an unfused aromatic system. The ELD and NMR spectroscopic data concur that DB669 behaves as a typical DNA-intercalating agent and binds equally well to AT and GC sites. It is somewhat surprising that DB669 fails to form minor-groove complexes with AT sites. The reason for that remains unclear at present; perhaps the radius of curvature of the molecule is not appropriate to allow the molecule to fit into the groove. This parameter is known to be important for the recognition of AT-containing sequences.[17, 18]

The situation is markedly different with the trithiophene compound, which has multiple binding modes. At low DNA/drug ratios, DB358 primarily binds to the minor groove of AT sequences in DNA. At high ratios DB358 appears to form intercalation complexes as suggested by upfield shifts in DB358 proton signals in NMR experiments at these ratios (data not shown). Thus, the sequence-dependent dual binding mode of DB60 is preserved. The use of complementary biophysical and footprinting techniques provides direct evidence that the AT and GC selectivity observed at low and high ratios are associated with minor-groove and intercalative binding, respectively. The substitution of the diphenylfuran moiety of DB60 with a trithiophene unit has reinforced significantly the capacity of the drug to engage in contacts with GC-containing sequences. DB358 only exhibits a mild preference for AT sequences. The SPR analysis indicates that the binding constant for DB358 to the alternating AT oligomer is only twofold higher than that for the alternating GC oligomer. The interaction of DB358 with sequences containing both A·T and G·C pairs is clearly evident from the footprinting studies. No such preferential interaction with GC-containing sites was observed with DB60.[10] The incorporation of thiophene heterocycles thus appears as a convenient procedure to limit the strict AT selectivity of dications containing an extended unfused aromatic system and to direct these imidazoline dications to GC-containing sites.

The study also shows that the replacement of the diphenylfuran core of DB60 with another aromatic system affects the capacity of the drug to interfere with the catalytic activity of human topoisomerase II. In our previous study, we detected a modest inhibition of topoisomerase II with DB60 but not with related AT-selective diphenylfurans containing amidine moieties. For this reason, we attributed the property of DB60 to stimulate DNA cleavage by topoisomerase II to its capacity to intercalate into GC sequences. The present data provide additional information which support the idea that topoisomerase II inhibition by aromatic dications is associated with GC binding. Indeed, the enhanced GC preference of DB358 compared to DB60 leads to a higher potency to inhibit topoisomerase II. In the relaxation assay, DB358 produces more double-strand breaks than the antitumor drug etoposide, which is a well-established poison for topoisomerase II. In the same assay, DB60 proved much less efficient than etoposide.[10] The fact that DB669 does not inhibit topoisomerase II was expected from its complete lack of GC preference, despite its intercalative binding. The terminal side chain plays a determinant role in the drug-induced stabilization of covalent DNA – topoisomerase II complexes.

Finally, the data suggest a relationship between topoisomerase II inhibition and cytotoxicity. Although DB358 may exert its cytotoxic effects by many different mechanisms, the increased capacity of DB358 to interact with GC-containing sequences and to inhibit topoisomerase II may account for the enhanced toxicity of the trithiophene towards leukemia cells compared to its trifuran counterpart. The search for GC binders targeted against topoisomerase II may thus represent a valid approach to the discovery of new antitumor agents. In this context, it is worth mentioning that recently Nieves-Neira et al.[19] discovered a topoisomerase-targeted drug active against human renal cancer

cells. This compound bears an unfused thiophen-furan-thiophen aromatic system that resembles a composite of DB358 and DB669.

Experimental Section

Chemical Syntheses

General: Melting points were recorded by using a Thomas Hoover (Uni-Melt) capillary melting point apparatus or a Fisher-Johns apparatus and are uncorrected. ^{1}H NMR and ^{13}C NMR spectra were recorded employing a Varian GX400 spectrometer and chemical shifts (δ) are given in ppm relative to TMS and coupling constants (J) are reported in Hertz. Mass spectra were recorded on a VG Instruments 70-SE spectrometer (Georgia Institute of Technology, Atlanta, GA). IR spectra were recorded using a Michelson 100 (Bomem, Inc.) instrument. Elemental analyses were obtained from Atlantic Microlab Inc. (Norcross, GA) and are within $\pm$0.4 of the theoretical values. All chemicals and solvents were purchased from Aldrich Chemical Co. or Fisher Scientific. 5′-Biotin-substituted hairpin DNA oligomers for SPR studies and DNA oligomer duplexes for NMR spectroscopy were obtained as HPLC-purified products from Midland Certified Reagent Co.

1,4-Di(4-bromo-2-thienyl)butadione (2): Divinyl sulfone (5.9 g, 0.05 mol) was added over a 2-h period to a stirred, refluxing mixture, under nitrogen, of 4-bromothiophene-2-carboxaldehyde (19.1 g, 0.01 mol), sodium acetate (1.86 g, 0.03 mol), 3-benzyl-5-hydroxyethyl-4-methylthiazolium chloride (2.69 g, 0.01 mol) in dry ethanol (75 mL). The mixture was heated under reflux for an additional 10 h. The mixture was cooled, the resultant solid was isolated by filtration and washed with cold ethanol. The light brown solid was dissolved in 500 mL of chloroform and chromatographed over silica gel to yield, after recrystallization from diethyl ether/chloroform (9:1), 6.9 g (33%) of an off-white solid. M.p. 142–143 °C; MS: m/z: 408 [M^+]; ^{1}H NMR ([D$_6$]DMSO): δ = 8.11 (d, 2H, J = 1.2 Hz), 8.08 (d, 2H, J = 1.2 Hz), 3.5 (s, 4H); ^{13}C NMR ([D$_6$]DMSO): δ = 190.8, 143.7, 134.8, 131.9, 109.8, 32.5.

2,5-Bis[2-(4-bromothienyl)]thiophene (3): A mixture of the 1,4-diketone **2** (4.08 g, 0.01 mol) and Lawesson's regent (4.04 g, 0.01 mol) in dry toluene (40 mL) was heated under reflux and under nitrogen for 4 h. The solvent was removed by distillation and the residue was suspended in water and extracted with warm chloroform (3 × 75 mL) and dried over Na_2SO_4. The organic phase was chromatographed over silica gel using chloroform as the eluant to yield 2.95 g (72%) of a yellow solid. M.p. 238–240 °C; MS: m/z: 406 [M^+]; ^{1}H NMR ([D$_6$]DMSO): δ = 7.54 (d, 2H, J = 1.5 Hz), 7.28 (d, 2H, J = 1.5 Hz), 7.26 (s, 2H); ^{13}C NMR ([D$_6$]DMSO): δ = 137.0, 134.5, 125.9, 125.5, 122.7, 109.4.

2,5-Bis[2-(4-cyanothienyl)]thiophene (4): A mixture of the dibromo compound **3** (2.03 g, 0.005 mol) and CuCN (1.99 g, 0.02 mol) in 10 mL of freshly distilled quinoline was heated, under reflux and under nitrogen, for 2 h. The mixture was cooled and 150 mL of chloroform was added. The chloroform solution was extracted with 2 M HCl (200 mL), and the organic layer was washed with water, dried, and passed through a neutral alumina column, using additional chloroform for elution to yield 0.9 g (60%) of a yellow solid. M.p. 174–176 °C; MS: m/z: 298 [M^+]; ^{1}H NMR ([D$_6$]DMSO): δ = 8.49 (d, 2H, J = 1.2 Hz), 7.73 (d, 2H, J = 1.2 Hz), 7.43 (s, 2H); ^{13}C NMR ([D$_6$]DMSO): δ = 137.4, 136.3, 134.2, 126.5, 124.8, 114.3, 110.1; elemental analysis (%): calcd for $C_{14}H_6N_2S_3$: C 56.34, H 2.02, N 9.39; found: C 56.21, H 2.11, N 9.28.

2,5-Bis{2-[4-(imidazolin-2-yl)thienyl]}thiophene (DB358): A mixture of the biscyano compound **4** (1.49 g, 0.005 mol) in 30 mL of dry ethanol was saturated with dry HCl gas at 0–5 °C. The mixture was stirred for 4 days at room temperature. Consumption of starting material was judged by disappearance of the nitrile band in the IR spectrum. The mixture was treated with dry diethyl ether and the imidate ester salt precipitated (2.15 g, 93%). The solid was isolated by filtration and dried under vacuum at 35 °C for 5 h. The imidate ester salt was used directly without characterization.

A suspension of the imidate ester salt (0.463 g, 0.001 mol) in 20 mL of dry ethanol and ethylenediamine (0.12 g, 0.002 mol) was heated under reflux for 12 h. The solvent was removed under reduced pressure, and the residue was washed with diethyl ether, dried, and dissolved in dry methanol and treated with dry HCl gas. The mixture was stirred for 3 h and diethyl ether was added. The resultant solid was washed with diethyl ether and dried under vacuum at 50 °C for 12 h to yield 0.33 g (71%). M.p. > 350 °C (decomp); MS (FAB): m/z: 385 [M^++1]; ^{1}H NMR ([D$_6$]DMSO/D$_2$O): δ = 8.4 (s, 2H), 7.73 (s, 2H), 7.33 (s, 2H), 3.95 (s, 8H); ^{13}C NMR ([D$_6$]DMSO/D$_2$O): δ = 160.1, 138.8, 135.3, 133.9, 127.3, 124.6, 123.1, 44.8; elemental analysis (%): calcd for $C_{18}H_{16}N_4S_3 \cdot 2\,HCl \cdot 0.5\,H_2O$: C 46.34, H 4.10, N 12.01; found: C 46.32, H 4.39, N 11.95.

2,5-Bis[2-(4-cyanofuranyl)]furan (5):[14] A mixture of 2,5-bis(tri-*n*-butylstannyl)furan (3.23 g, 0.055 mol), 2-bromo-4-cyanofuran[20] (1.72 g, 0.01 mol), and [Pd(PPh$_3$)$_4$] (0.28 g, 2.5 mol%) in 60 mL of dry dioxane was heated, under reflux and under nitrogen, for 12 h. The solvent was removed under reduced pressure. The residue was dissolved in *n*-hexane and chromatographed over neutral alumina, first by eluting with *n*-hexane to remove butyltin compounds and finally with benzene/*n*-hexane (1:9) to yield 0.85 g (69%) of a yellow solid. M.p. 212–213; MS: m/z: 250 [M^+]; ^{1}H NMR ([D$_6$]DMSO): δ = 8.70 (d, 2H, J = 0.8 Hz), 7.24 (d, 2H, J = 0.8 Hz), 7.03 (s, 2H); ^{13}C NMR ([D$_6$]DMSO): δ = 151.4, 145.9, 143.7, 112.7, 109.9, 106.7, 98.6; elemental analysis (%): calcd for $C_{14}H_6N_2O_3$: C 67.20, H 2.41, N 11.19; found: C 66.98, H 2.50, N 10.92.

2,5-Bis{2-[4-(imidazolin-2-yl)furanyl]}furan (DB669): A mixture of the biscyano compound **5** (0.7 g, 0.0028 mol) in 25 mL of dry ethanol was saturated with dry HCl gas at 0–5 °C. The mixture was stirred for 6 days at room temperature. Consumption of starting material was judged by the disappearance of the nitrile band in the IR spectrum. The mixture was treated with dry diethyl ether and the imidate ester salt precipitated. The solid was isolated by filtration and dried under vacuum at 40 °C for 8 h to yield 1.0 g (86%). The imidate ester salt was used directly without characterization.

A suspension of the imidate ester salt (0.415 g, 0.001 mol) in 15 mL of dry ethanol and ethylenediamine (0.12 g, 0.002 mol) was heated under reflux for 12 h. The solvent was removed under reduced pressure and the residue was washed with ether, dried, and dissolved in dry methanol and treated with dry HCl gas. The mixture was stirred for 3 h and diethyl ether was added. The resultant solid was washed with diethyl ether and dried under vacuum at 50 °C for 12 h to yield 0.33 g (79%). M.p. > 330 °C (decomp); MS (FAB): m/z: 337 [M^++1]; ^{1}H NMR ([D$_6$]DMSO/D$_2$O): δ = 8.62 (d, 2H, J = 0.4 Hz), 7.28 (d, 2H, J = 0.4 Hz), 7.01 (s, 2H), 3.9 (s, 8H); ^{13}C NMR ([D$_6$]DMSO/D$_2$O): δ = 159.0, 148.4, 147.0, 144.4, 112.7, 110.7, 104.6, 44.6; elemental analysis (%): calcd for $C_{18}H_{16}N_4O_3 \cdot 2\,HCl \cdot 0.5\,H_2O$: C 51.66, H 4.58, N 13.39; found: C 51.64, H 4.67, N 13.45.

Chemicals and biochemicals: Etoposide and camptothecin were purchased from Sigma Chemical Co. Calf thymus DNA and the double-stranded polymers poly(d(AT))·poly(d(AT)) and poly(d(GC))·poly(d(GC)) were obtained from Pharmacia. Calf thymus DNA was deproteinized with sodium dodecylsulfate (SDS; protein content

$< 0.2\%$). The nucleoside triphosphate labeled with [α-^{32}P]dATP was obtained from Amersham (3000 Ci mmol^{-1}). Restriction endonucleases and avian myeloblastosis virus (AMV) reverse transcriptase were purchased from Boehringer and used according to the supplier's recommended protocol in the activity buffer provided. All other chemicals were analytical-grade reagents.

Absorption spectroscopy and DNA thermal melting studies: UV/Vis scans and T_m values were obtained with Cary 3 and 4 spectrometers in 2-(*N*-morpholino)ethanesulfonic acid (MES) buffer (0.01 M MES and 10^{-3} M ethylenediaminetetraacetic acid (EDTA)) with 0.1 M NaCl added. A thermistor fixed into a reference cuvette was used to monitor the temperature. In T_m experiments DNA was added to the buffer in 1-cm path length reduced-volume quartz cells, and the concentration was determined by measuring the absorbance at 260 nm. The experiments were generally conducted at a concentration of 5×10^{-5} M base pairs for all DNAs and a compound/DNA base pair ratio of 0.6. In spectrophotometric titrations the compound was added to the buffer in a 1-cm cell and DNA was titrated in at a variety of ratios with rescanning at each ratio.

Biosensor surface plasmon resonance (SPR) studies: SPR measurements were performed with a four-channel BIAcore 2000 system and streptavidin-coated sensor chips. 5′-Biotinylated hairpin DNAs (25 nM) of the desired sequence in MES buffer with 0.1 M NaCl were immobilized on the surface by noncovalent capture. Three flow cells were used to immobilize DNA samples and the fourth flow cell was left as a blank control. Samples of the drug were prepared in filtered and degassed buffer and were injected from 7-mm plastic vials with pierceable plastic crimp caps at a flow rate of 20 μL min^{-1} by using the KINJECT command. For the DNA complexes in this work buffer flow alone is sufficient to dissociate the compounds from the DNA for surface regeneration. A range of compound concentrations was used in each experiment and the results were analyzed according to Equation (1):

$$r = (nKC_{free}/(1 + KC_{free}) \quad (1)$$

where r (moles of compound bound per mole of hairpin) $= RU/RU_{max}$, RU (resonance units) represents the instrument response at any compound concentration, $n = 3$ for a three-site model, and RU_{max} is the maximum response per site.[21] The K values are equilibrium constants for a three-site binding model, and C_{free} is the concentration of unbound compound that is fixed by the concentration in the flow solution. For models with fewer binding sites, n can be set to lower values.

Circular dichroism (CD) spectroscopy: CD spectra were obtained on a Jasco J-710 spectrometer with software supplied by Jasco for instrument control and data acquisition. A solution of the desired DNA was scanned, the compound added, and the sample rescanned at all desired ratios. Studies with poly(d(A-T)$_2$) and calf thymus DNA were done in MES with 0.1 M NaCl, and studies with poly(d(G-C)$_2$) were done in MES buffer with no added salt.

Electric linear dichroism (ELD) spectroscopy: Measurements were performed with a computerized optical measurement system using the procedures previously outlined.[22] All experiments were conducted with a 10-mm pathlength Kerr cell having 1.5 mm electrode separation. The samples were oriented under an electric field strength varying from 1 to 13 kV cm^{-1}. The drug tested was present at 10 μM concentration together with the DNA at 200 μM concentration unless otherwise stated. This electro-optical method has proved most useful to determine the orientation of the drugs bound to DNA. It has the additional advantage that it senses only the orientation of the polymer-bound ligand: Free ligand is isotropic and does not contribute to the signal.[23]

NMR spectroscopy of DB358: A 1D NMR study of DB358 with the oligomers (A-T)$_7$ and (G-C)$_7$ was done with 0.5 mM DB358 in 0.6 mL of phosphate buffer (7.5 mM sodium phosphate, 100 mM NaCl, and 0.01 mM EDTA, pH 7.0). After addition of an appropriate volume of oligomer stock solution (to achieve the desired DNA/drug ratio), the solvent was removed under N_2 and 0.4 mL of 99.96% D_2O (Isotec) was added. Solvent was removed twice in order to minimize the amount of HDO and a final volume of 0.6 mL of 99.96% D_2O was added. Studies were done on Varian Unity + 500- and 600-MHz NMR instruments and data were processed using the Felix software package running on a Silicon Graphics workstation. The two-dimensional experiments were obtained with a spectral width of 6000 Hz in both dimensions with 2048 complex data points in the t_2 dimension and 512 points in the t_1 dimension. Phase-sensitive NOESY spectra were obtained with a mixing time of 300 ms by using the method of States et al.[24]

Molecular modeling: Preoptimization of all compounds was done using the Spartan software package (version 5.0, Wavefunction, Inc.). The minimized models were docked with DNA and minimized with the SYBYL software package (version 6, Tripos). The DNA model was obtained from a previously determined crystal structure for furamidine with the compound used as a docking guide and then deleted.[25] Several distances were monitored in real time in the SYBYL software during visual docking: hydrogen bond lengths from DB358 amidines to the same DNA positions as in the furamidine structure, and DB358 proton to DNA proton distances that give NOE cross peaks in NOESY 2D spectra. A model was selected that gave optimum values for all of these distances prior to energy minimization. No constraints were used in the energy minimization of the model shown in Figure 7, but all of the above distances remained close to the initial values in the minimization.

DNA purification and radiolabeling: The 117-mer and 265-mer fragments were rendered radioactive by [^{32}P]-3′-end labeling of the *Eco*RI – *Pvu*II double digest of the plasmid pBS (Stratagene, La Jolla, CA) using [α-^{32}P]dATP (3000 Ci mmol^{-1}) and AVM reverse transcriptase. The labeled digestion products were separated on a 6% (w/v) polyacrylamide gel under nondenaturing conditions in TBE buffer (89 mM Tris-borate, pH 8.3, 1 mM EDTA). After autoradiography, the requisite band of DNA was excised, crushed, and soaked in elution buffer (500 mM ammonium acetate, 10 mM magnesium acetate) overnight at 37 °C. This suspension was filtered through a Millipore 0.22-μm filter and the DNA was precipitated with ethanol. Following washing with 70% ethanol and vacuum drying of the precipitate, the labeled DNA was resuspended in 10 mM Tris adjusted to pH 7.0 containing 10 mM NaCl.

DNase I footprinting: Experiments were performed essentially as previously described.[15] Briefly, reactions were conducted in a total volume of 10 μL. Samples (3 μL) of the labeled DNA fragments were incubated with 5 μL of the buffered solution containing the ligand at appropriate concentration. After 30 min incubation at 37 °C to ensure equilibration of the binding reaction, the digestion was initiated by the addition of 2 μL of a DNase I solution whose concentration was adjusted to yield a final enzyme concentration of about 0.01 U mL^{-1} in the reaction mixture. After 3 min, the reaction was stopped by freeze drying. Samples were lyophilized and resuspended in 5 μL of an 80% formamide solution containing tracking dyes. The DNA samples were then heated at 90 °C for 4 min and chilled on ice for 4 min prior to electrophoresis.

Electrophoresis and quantitation by storage phosphor imaging: DNA cleavage products were resolved by polyacrylamide gel

electrophoresis under denaturating conditions (0.3 mm thick, 8% (w/v) acrylamide containing 8 M urea). After electrophoresis (about 2.5 h at 60 W, 1600 V in Tris/borate/EDTA-buffered solution, BRL sequencer model S2), gels were soaked in 10% acetic acid for 10 min, transferred to Whatman 3MM paper, and dried under vacuum at 80 °C. A Molecular Dynamics 425E PhosphorImager was used to collect data from the storage screens exposed to dried gels overnight at room temperature. Base-line-corrected scans were analyzed by integrating all the densities between two selected boundaries using ImageQuant version 3.3 software. Each resolved band was assigned to a particular bond within the DNA fragments by comparison of its position relative to sequencing standards generated by treatment of the DNA with dimethylsulfate followed by piperidine-induced cleavage at the modified guanine bases in DNA (G track).

DNA relaxation experiments: Supercoiled pKMp27 DNA (0.5 μg) was incubated with 4 units of human topoisomerase I or II (TopoGen, Inc.) at 37 °C for 1 h in relaxation buffer (50 mM Tris, pH 7.8, 50 mM KCl, 10 mM $MgCl_2$, 1 mM dithiothreitol, 1 mM EDTA, 1 mM ATP) in the presence of varying concentrations of the drug under study. Reactions were terminated by adding SDS to 0.25% (w/v) and proteinase K to 250 μg mL^{-1}. DNA samples were then added to the electrophoresis dye mixture (3 μL) and electrophoresed in an ethidium-containing 1% agarose gel at room temperature for 2 h at 120 V (10 V cm^{-1}). Gels were washed and photographed under UV light.

Cell cultures and survival assay: Human HL-60 promyelocytic leukemia cells were obtained from the American Tissue Culture Collection (Manassas, VA). Cells were grown at 37 °C in a humidified atmosphere containing 5% CO_2 in RPMI 1664 medium, supplemented with 10% fetal bovine serum, glutamine (2 mM), penicillin (100 IU mL^{-1}), and streptomycin (100 μg ml^{-1}). The cytotoxicity of the drugs was assessed by using a cell proliferation assay developed by Promega (CellTiter 96 AQ_{ueous} one solution cell proliferation assay). Briefly, 2×10^4 exponentially growing cells were seeded in 96-well microculture plates with various drug concentrations in a volume of 100 μL. After 72 h incubation at 37 °C, 20 μL of MTS (3-(4,5-dimethylthiazol-2-yl)-5-(3-carboxymethoxyphenyl)-2-(4-sulfophenyl)-2*H*-tetrazolium, inner salt) were added to each well and the samples were incubated for a further 3 h at 37 °C. Plates were analyzed on a Labsystems Multiskan MS (type 352) reader at 492 nm.

Cell cycle analysis: For flow cytometric analysis of DNA content, 10^6 HL-60 cells in exponential growth were treated with graded concentrations of the test drug for 24 h and then washed three times with citrate buffer. The cell pellet was incubated with 250 μL of trypsin-containing citrate buffer for 10 min at room temperature and then with 200 μL of citrate buffer containing a trypsin inhibitor and RNase (10 min) prior to adding 200 μL of propidium iodide (PI) at 125 μg mL^{-1}. Samples were analyzed on a Becton Dickinson FACScan flow cytometer using the LYSYS II software, which was also used to determine the percentage of cells in the different phases of the cell cycle. PI was excited at 488 nm, and fluorescence analyzed at 620 nm (using channel Fl-3).

This work was done under the support of research grants (to C.B.) from the Institut de Recherches sur le Cancer de Lille (IRCL) and the Ligue Nationale Contre le Cancer (Comité du Nord); (to W.D.W. and D.W.B.) from NIH grant GM61587 and the Georgia Research Alliance; (to P.B.) by a Fulbright Fellowship from the Fulbright Commission of the Czech Republic; (to C.H. and P.C.) from the Actions de Recherches Concertées, contract n°95/00 – 93. Support by the convention INSERM-CFB is acknowledged.

[1] B. P. Das, D. W. Boykin, *J. Med. Chem.* **1977**, *20*, 531 – 536.
[2] E. A. Steck, K. K. Kinnamon, D. E. Davidson, R. E. Duxbury, A. J. Johnson, R. E. Masters, *Exp. Parasitol.* **1982**, *53*, 133 – 144.
[3] D. W. Boykin, A. Kumar, J. Spychala, M. Zhou, R. L. Lombardi, W. D. Wilson, C. C. Dykstra, S. K. Jones, J. E. Hall, R. R. Tidwell, C. Laughton, C. M. Nunn, S. Neidle, *J. Med. Chem.* **1995**, *38*, 912 – 916.
[4] D. W. Boykin, A. Kumar, G. Xiao, W. D. Wilson, B. C. Bender, D. R. McCurdy, J. E. Hall, R. R. Tidwell, *J. Med. Chem.* **1998**, *41*, 124 – 129.
[5] I. Francesconi, W. D. Wilson, F. A. Tanious, J. E. Hall, B. C. Bender, R. R. Tidwell, D. McCurdy, D. W. Boykin, *J. Med. Chem.* **1999**, *42*, 2260 – 2265.
[6] S. Neidle, L. R. Kelland, J. O. Trent, I. J. Simpson, D. W. Boykin, A. Kumar, W. D. Wilson, *Bioorg. Med. Chem.* **1997**, *7*, 1403 – 1408.
[7] J. O. Trent, G. R. Clark, A. Kumar, W. D. Wilson, D. W. Boykin, J. E. Hall, R. R. Tidwell, B. L. Blagburn, S. Neidle, *J. Med. Chem.* **1996**, *39*, 4554 – 4562.
[8] R. L. Lombardi, F. A. Tanious, K. Ramachandran, R. R. Tidwell, W. D. Wilson, *J. Med. Chem.* **1996**, *39*, 1452 – 1462.
[9] W. D. Wilson, F. A. Tanious, D. Ding, A. Kumar, D. W. Boykin, P. Colson, C. Houssier, C. Bailly, *J. Am. Chem. Soc.* **1998**, *120*, 10310 – 10321.
[10] C. Bailly, L. Dassonneville, C. Carrasco, D. Lucas, A. Kumar, D. W. Boykin, W. D. Wilson, *Anti-Cancer Drug Des.* **1999**, *14*, 47 – 60.
[11] L. Wang, C. Bailly, A. Kumar, D. Ding, M. Bajic, D. W. Boykin, W. D. Wilson, *Proc. Natl. Acad. Sci. USA* **2000**, *97*, 12 – 16.
[12] M. Bajic, A. Kumar, D. W. Boykin, *Heterocycl. Commun.* **1996**, *2*, 135 – 138.
[13] M. P. Cava, M. I. Levinson, *Tetrahedron* **1985**, *41*, 5061 – 5087.
[14] A. Kumar, C. E. Stephens, D. W. Boykin, *Heterocycl. Commun.* **1999**, *5*, 301 – 304.
[15] C. Bailly, M. J. Waring, *J. Biomol. Struct. Dyn.* **1995**, *12*, 869 – 898.
[16] J. Kluza, A. Lansiaux, N. Wattez, C. Mahieu, N. Osheroff, C. Bailly, *Cancer Res.* **2000**, *60*, 4077 – 4084.
[17] R. R. Tidwell, S. K. Jones, J. D. Geratz, K. A. Ohemeng, M. Cory, J. E. Hall, *J. Med. Chem.* **1990**, *33*, 1252 – 1257.
[18] M. Cory, R. R. Tidwell, T. A. Fairley, *J. Med. Chem.* **1992**, *35*, 431 – 438.
[19] W. Nieves-Neira, M. I. Rivera, G. Kohlhagen, M. L. Hursey, P. Pourquier, E. A. Sausville, Y. Pommier, *Mol. Pharmacol.* **1999**, *56*, 478 – 484.
[20] G. Johansson, S. Sundquist, G. Nordvall, B. M. Nilsson, M. Brisander, L. Nilvebrant, U. Hacksell, *J. Med. Chem.* **1997**, *40*, 3804 – 3819.
[21] T. M. Davis, W. D. Wilson, *Anal. Biochem.* **2000**, *284*, 348 – 353.
[22] C. Houssier in *Molecular Electro-Optics* (Ed.: S. Krause), Plenum, New York, **1981**, pp. 363 – 398.
[23] P. Colson, C. Bailly, C. Houssier, *Biophys. Chem.* **1996**, *58*, 125 – 140.
[24] D. J. States, R. A. Haberkorn, D. J. Ruben, *J. Magn. Reson.* **1982**, *48*, 286 – 292.
[25] C. Laughton, F. Tanious, C. M. Nunn, D. W. Boykin, W. D. Wilson, S. Neidle, *Biochemistry* **1996**, *35*, 5655 – 5661.

Received: September 29, 2000 [F 140]